

Structural properties of undoped and doped with Er³⁺ ions ZnGa₂O₄ nanomaterials obtained by hydrothermal method

M. VASILE*, C. IANASI^a, A. - V. BÎRDEANU^b, E. VASILE^c

National Institute for Research and Development in Electrochemistry and Condensed Matter Timisoara, 300224, Romania

^aInstitute of Chemistry Timisoara of Romanian Academy, 300223, Timisoara, Romania

^bNational R&D Institute for Welding and Material Testing - ISIM Timisoara 300222, Timisoara, Romania

^cMetav S.A., Bucharest, Romania

Erbium-doped nanosized ZnGa₂O₄ phosphors with the nominal formula of ZnGa_{2-x}O₄:xEr (x=0.05 and 0.01) were synthesized by hydrothermal method. The crystal structures were investigated by means X-ray diffraction experiments were carried out on a PANalytical X'Pert Pro diffractometer equipped with an Anton Paar HTK2000 high-temperature camera, transmission electron microscope (TEM) and BET (Brunauer Emmett Teller). An X-ray diffraction spectrum was made up to a temperature of 500°C and does not change form of crystallization. The results, from TEM measurements, indicate that the material consisting of ZnGa_{2-x}O₄:xEr particles exhibits good crystallinity with cubic spinel structure and the particle size varies with the quantity of doping. The surface area (S_{BET}) of ZnGa_{2-x}O₄:xEr (x=0.05 and 0.01) increases compared with undoped ZnGa₂O₄.

(Received October 5, 2011; accepted October 20, 2011)

Keywords: Phosphors, Erbium, Nanomaterials

1. Introduction

The luminescent characteristics of inorganic ZnGa₂O₄ phosphors have been extensively investigated for commercial: FEDs (field emission displays) have recently gained much attention as they are considered next generation flat panel displays, especially of great interest are SEDs (surface-conduction electron-emitter displays) which are the type of FED, because of their relative ease of fabrication (no emitter tips) and low energy consumption, the energy consumption of SEDs is even lower than that of CRTs, their energy consumption depends very much on the emission efficiency of phosphors [1–10]. Spinel oxides form an important range of ceramic compounds with great interesting electrical, mechanical, magnetic and optical properties. It is observe that wide band gaps in these structures offer attractive photoelectronic and optical applications [11].

ZnGa₂O₄ has a normal spinel crystal structure with *Fd3m* space group. The normal spinel ZnGa₂O₄ has tetrahedrally coordinated Zn sites (Td) surrounded by four oxygen atoms and octahedrally coordinated Ga sites (Oh) surrounded by six oxygen atoms. The 32 oxygen ions are C_{3v} sites arranged in a close-packed cubic formation leaving 64 tetrahedral (Td) and 32 distorted (D_{3d}) sites [12]. Its optical band gap is approximately 4.4 eV [13]. Moreover, these compounds are highly reflective for wavelengths in (UV) regions, which make them candidate materials for reflective optical coating in aerospace applications [14].

Doped or undoped ZnGa₂O₄ phosphors show less out gassing and more chemically stable properties than those of sulfide phosphors [15, 16]. Mn²⁺-doped ZnGa₂O₄ phosphor exhibits an intense green emission peaking at 505 nm [16]. Cr³⁺-doped ZnGa₂O₄ phosphor emits red light of 700 nm [17,18]. Undoped ZnGa₂O₄ phosphor shows a blue emission band around 430 nm when it is synthesized in an oxidizing ambient, whereas it shows an ultraviolet emission band around 360 nm when it is annealed in a reducing ambient [19]. Like other wide band gap semiconductors, ZnGa₂O₄ exhibits a blue emission under excitation by both ultraviolet light and low-voltage electrons. Activation with Mn²⁺ or Er³⁺ ions shifts the emission to green or red [20 - 23].

In this work, nanosized Er³⁺-doped ZnGa₂O₄ phosphors with the nominal formula of ZnGa_{2-x}O₄:xEr were synthesized by hydrothermal method and the made investigations of thermally stable and the crystal structure properties were investigated.

2. Experimental procedure

For synthesis by hydrothermal method of the ZnGa₂O₄ and ZnGa_{2-x}O₄:xEr with x = 0.05 and 0.01 were using precursors: zinc nitrate Zn(NO₃)₂*6H₂O (99.99%, Merck), gallium-oxide Ga₂O₃ (99.99%, Aldrich,) and erbium-oxide Er₂O₃ (99.99%, Aldrich) respecting the molar ratio 1:1. The resulting mixture was

then adjusted to a special pH ~ 12 with sodium hydroxide solution under vigorous stirring.

After drying, the characterization of the obtained material was achieved by X-ray powder diffractometer (PANalytical X'Pert Pro) with monochromatic Cu K α ($k = 1.5418 \text{ \AA}$) incident radiation. Diffractograms were collected during heating and cooling using a Anton-Paar HTK2000 high-temperature camera furnace equipped with a Pt strip heater. For the identification of the morphology were used Transmission Electron Microscopy (TEM) TECNAI F30 G2 with 1 \AA linear resolution and a resolution of 1.4 \AA . BET method (Brunauer, Emmett, Teller) [24] is the method used to estimate the specific surface. This method can cause a number of parameters describing the porous structure of solid materials, such as surface area, volume and pore size. Determination of active surface was achieved with Micrometrics ASAP 2020 instrument. To perform these measurements, the samples were degassed to measure specific surface under the following conditions: temperature of the landing 1500°C , the pressure of the landing $10 \mu\text{mcol.Hg}$, the time of the landing 180 min .

3. Results and discussions

Fig. 1 shows the Anton-Paar HTK2000 high-temperature camera spectra of the undoped and doped ZnGa_2O_4 with of Er^{3+} ions ($\text{ZnGa}_{2-x}\text{O}_4 : x\text{Er}$ ($x = 0.05$ and 0.01)). These spectra were made at different temperatures ranging from 25°C and then 50°C in 50°C up to 500°C . The XRD spectra exhibit broadened diffraction peaks indicating the nanocrystalline nature. All the peaks can be perfectly indexed with crystalline ZnGa_2O_4 phase (JCPDS, card No. 86-0415). The peaks of the XRD spectrums for ZnGa_2O_4 doped with Er^{3+} ($\text{ZnGa}_{2-x}\text{O}_4 : x\text{Er}$ ($x = 0.05$ and 0.01)) ions show a slight shift to the left compared with the peaks of the undoped ZnGa_2O_4 . XRD patterns of the powder phosphors formed showed ZnGa_2O_4 and ZnGa_2O_4 doped with Er^{3+} ($\text{ZnGa}_{2-x}\text{O}_4 : x\text{Er}$ ($x = 0.05$ and 0.01)) ions crystalline phases of spinel structure in which the (3 1 1) plane indicating the standard powder diffraction pattern of ZnGa_2O_4 phase and the (2 2 0) peak of preferred orientation of powder were detected. All the specimens showed (3 1 1) peak with highest intensity in the XRD patterns. The diffraction peaks in the patterns are indexed to spinel (space group $Fd\bar{3}m$) phases. The intensity of the peaks relative to the background signal demonstrates high purity and good quality of the samples.

The mean crystallite size (d) of the powder samples was calculated using Scherrer's formula [25]:

$$d = \frac{K\lambda}{(\beta^2 - \beta_0^2)^{1/2}} \cos\theta$$

where β is the half-width of the diffraction peak in radians, β_0 corresponds to the instrumental broadening, $K = 180/\pi$, λ is the X-ray wavelength, and θ is the Bragg diffraction angle. The average crystallite size determined from XRD line broadening is $\sim 50 \text{ nm}$ for $\text{ZnGa}_{2-x}\text{O}_4 : x\text{Er}^{3+}$ ($x=0.05$) and $\sim 35 \text{ nm}$ for $\text{ZnGa}_{2-x}\text{O}_4 : x\text{Er}^{3+}$ ($x=0.01$). The lattice constant was calculated from XRD results, using FullProf Suite computer package, the values obtained being: $a = 8.35675 \text{ \AA}$ for $\text{ZnGa}_{2-x}\text{O}_4 : x\text{Er}^{3+}$ ($x=0.05$) and $a = 8.35671 \text{ \AA}$ for $\text{ZnGa}_{2-x}\text{O}_4 : x\text{Er}^{3+}$ ($x=0.01$).

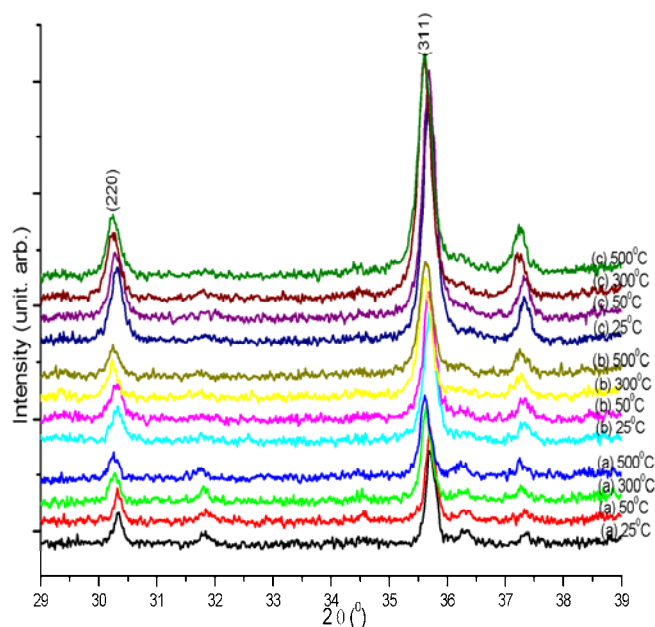


Fig. 1. HTK2000 high-temperature camera spectra at 25°C , 50°C , 300°C and 500°C of (a) undoped ZnGa_2O_4 , (b) $\text{ZnGa}_{2-x}\text{O}_4 : x\text{Er}^{3+}$ ($x=0.05$), and (c) $\text{ZnGa}_{2-x}\text{O}_4 : x\text{Er}^{3+}$ ($x=0.01$).

The morphological aspect of the resulting powders ZnGa_2O_4 and $\text{ZnGa}_{2-x}\text{O}_4 : x\text{Er}$ ($x = 0.05$ and 0.01) was examined by TEM, as shown in Figure 2 (a, b and c). Fig. 2 (b and c) illustrates that the particles have a regular shape, but their size varies for $\text{ZnGa}_{2-x}\text{O}_4 : x\text{Er}^{3+}$ ($x=0.05$) is between $70\text{-}20 \text{ nm}$ and for $\text{ZnGa}_{2-x}\text{O}_4 : x\text{Er}^{3+}$ ($x=0.01$) is between $50\text{-}10 \text{ nm}$. This result is inconsistent with the size calculated by Scherrer's equation in the XRD pattern illustrated in Figure 1. From these measures is seen as the cubic form at undoped ZnGa_2O_4 and $\text{ZnGa}_{2-x}\text{O}_4 : x\text{Er}$ ($x = 0.05$ and 0.01) nanoparticles. The nanoparticle size of ZnGa_2O_4 doped with Er^{3+} ions is smaller than the undoped ZnGa_2O_4 . The particle sizes depends on the concentration of dopant used. The dependence of particle size is directly proportional to the concentration of impurity used in the synthesis.

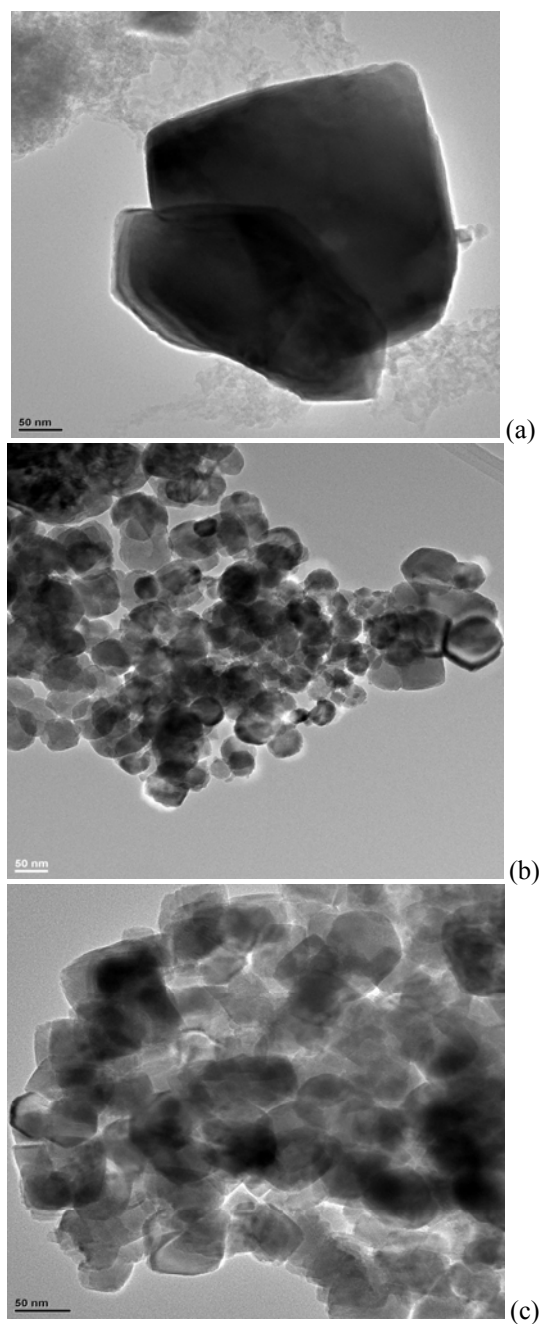


Fig. 2 TEM image of (a) undoped ZnGa_2O_4 , (b) $\text{ZnGa}_{2-x}\text{O}_4 : x\text{Er}^{3+}$ ($x=0.05$), and (c) $\text{ZnGa}_{2-x}\text{O}_4 : x\text{Er}^{3+}$ ($x=0.01$).

Fig. 3(a, b and c) shows the HRTEM images of undoped and doped ZnGa_2O_4 with of Er^{3+} ions ($\text{ZnGa}_{2-x}\text{O}_4 : x\text{Er}$ ($x = 0.05$ and 0.01)) nanoparticles. Two-dimensional lattice fringes can be seen clearly in the HRTEM image, which indicates that undoped ZnGa_2O_4 and $\text{ZnGa}_{2-x}\text{O}_4 : x\text{Er}$ ($x = 0.05$ and 0.01)) particles have good crystallinity and the nanoparticle is composed of several small crystallites.

Besides, to make clear the intrinsic structures of these undoped ZnGa_2O_4 and $\text{ZnGa}_{2-x}\text{O}_4 : x\text{Er}$ ($x = 0.05$ and 0.01)) phosphors, we carried out HRTEM analysis. The corresponding HRTEM image in Figure 3 (a, b and c) are clear lattice fringes and also exhibits bright-dark field,

indicating the high crystallinity and mesoporous structures, respectively. Meanwhile, the lattice spacing shown in Figure 3 (a) is of ca. 0.29 nm, corresponding to that of (220) plane of undoped ZnGa_2O_4 sample, in Figure 3 (b) is of ca. 0.17 nm, corresponding to that of (422) plane and for ca. 0.25 nm, corresponding to that of (311) plane of $\text{ZnGa}_{2-x}\text{O}_4 : x\text{Er}^{3+}$ ($x=0.05$) and in Figure 3 (c) is of ca. 0.16 nm, corresponding to that of (511) plane of $\text{ZnGa}_{2-x}\text{O}_4 : x\text{Er}^{3+}$ ($x=0.01$).

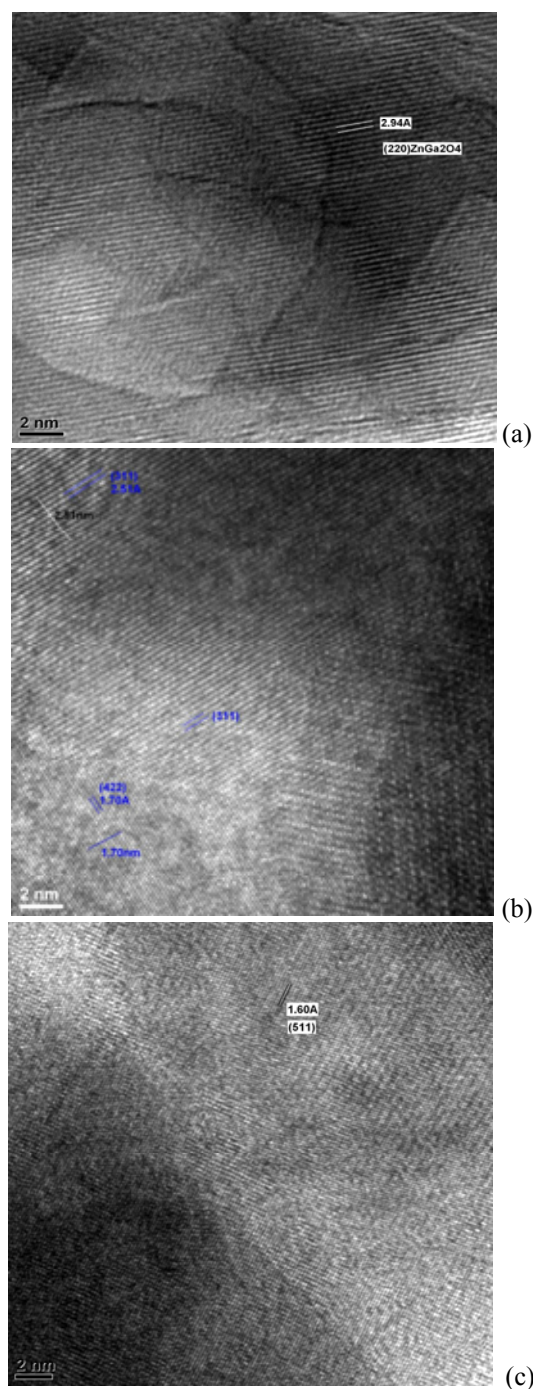


Fig. 3. HRTEM images of (a) undoped ZnGa_2O_4 , (b) $\text{ZnGa}_{2-x}\text{O}_4 : x\text{Er}^{3+}$ ($x=0.05$), and (c) $\text{ZnGa}_{2-x}\text{O}_4 : x\text{Er}^{3+}$ ($x=0.01$).

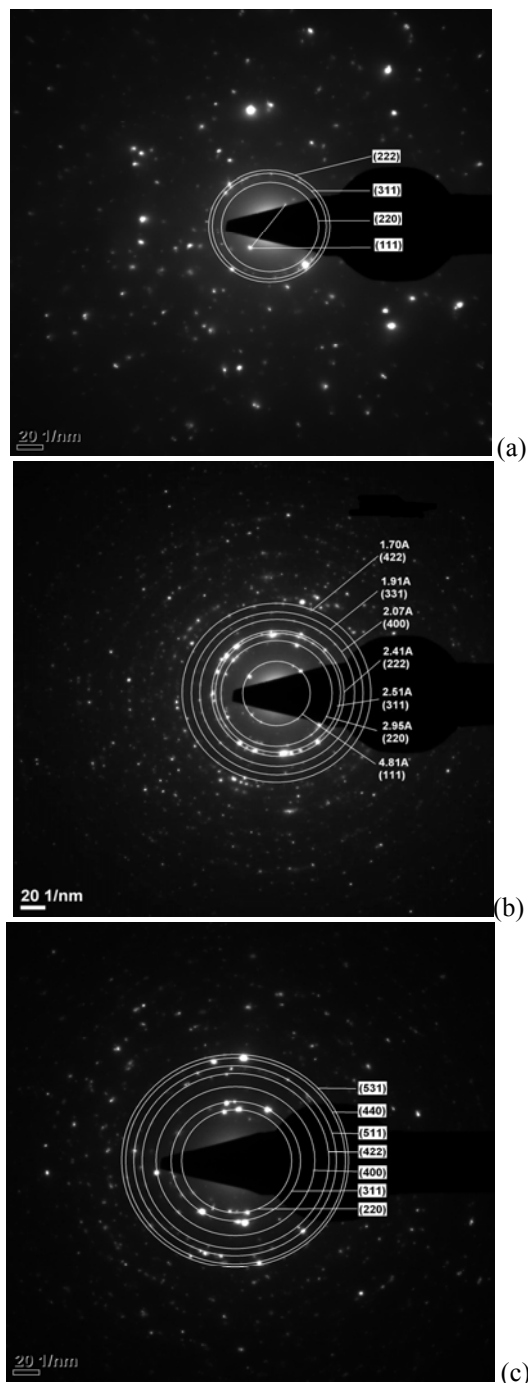


Fig. 4. SAED images of (a) undoped $ZnGa_2O_4$, (b) $ZnGa_{2-x}O_4 : xEr^{3+}$ ($x=0.05$), and (c) $ZnGa_{2-x}O_4 : xEr^{3+}$ ($x=0.01$).

Electron diffraction (SAED) images in Figure 4 (a, b and c) are associated nanozonolite in Figure 2. Diffraction circles marked with diameters correspond to interplanar distances specific to crystal plane families (indexed image) of undoped and doped $ZnGa_2O_4$ with Er^{3+} ions with cubic lattice with centered faces. In these images of the electron diffraction (SAED) appear preferentially crystallographic planes, as in Figure 4 (a) shows the electrons diffraction are highlighted of the undoped $ZnGa_2O_4$ crystallographic planes (111), (220), (311) and (222). Doped the materials with Er^{3+} ions, the particle size is smaller, could reveal

more crystallographic plane. Fig. 4 (b) shows the SAED of $ZnGa_{2-x}O_4 : xEr^{3+}$ ($x=0.05$) which can be seen crystallographic planes (422), (331), (400), (222), (311), (220) and (111). In the electron diffraction (SAED) images of $ZnGa_{2-x}O_4 : xEr^{3+}$ ($x=0.01$) (Figure 4 (c)) are identified these crystallographic planes (531), (440), (511), (422), (400), (311) and (220). Can see that in all cases appear crystallographic planes (220) and (311) which confirms measurements XRD.

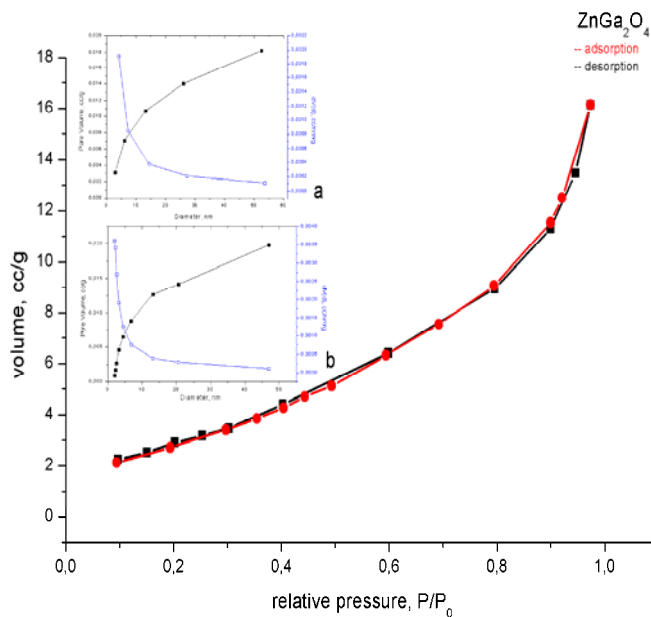


Fig. 5. Adsorption/desorption isotherms of N_2 at 77 K for undoped $ZnGa_2O_4$. Inset shows pore size of: a) BJH adsorption and b) BJH desorption

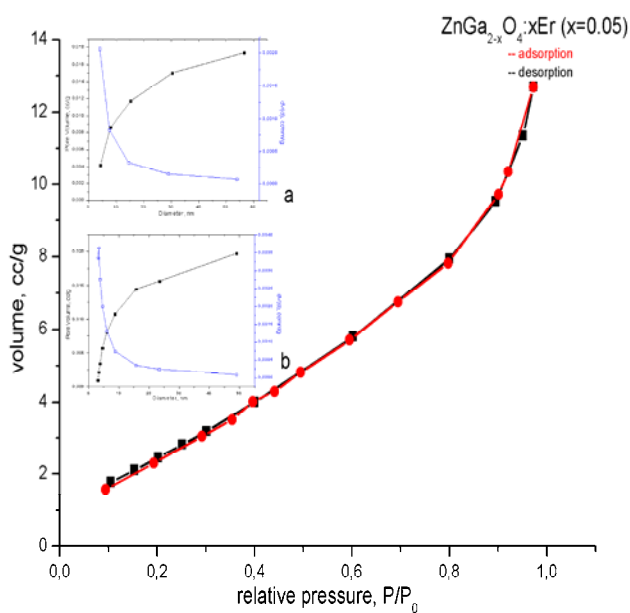


Fig. 6 Adsorption/desorption isotherms of N_2 at 77 K for $ZnGa_{2-x}O_4 : xEr^{3+}$ ($x=0.05$). Inset shows pore size of: a) BJH adsorption and b) BJH desorption

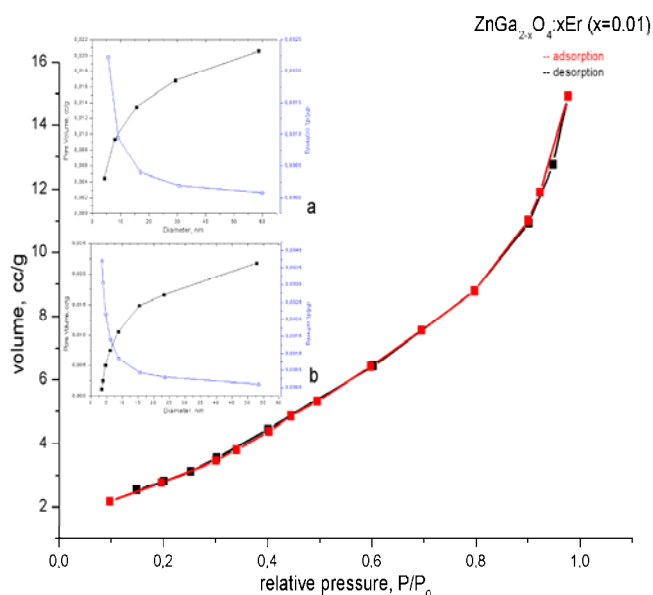


Fig. 7 Adsorption/desorption isotherms of N₂ at 77 K for ZnGa_{2-x}O₄:xEr³⁺ (x=0.01). Inset shows pore size of: a) BJH adsorption and b) BJH desorption

Figs. 5, 6 and 7 exhibits a type IV (accordance with standard IUPAC) adsorption–desorption isotherms, which is typically characteristic of mesoporous materials. We also find out that the hysteresis loop appears at high pressure of $0.60 < P/P_0 < 0.98$, revealing the presence of irregular large pores. All the isotherms presented in Figures 5, 6 and 7 are the type inkbottle. And the surface area of the spherical porous ZnGa₂O₄, ZnGa_{2-x}O₄:xEr³⁺ (x=0.05) and ZnGa_{2-x}O₄:xEr³⁺ (x=0.01) phosphors is presented in Table 1 by the Brunauer–Emmett–Teller (BET) equation. For graphics inserted in Figure 5 (a and b), Fig. 6 (a and b) and Fig. 7 (a and b) or could calculate the average pore radius. These results are presented in Table 1.

The porous nature of the ZnGa₂O₄, ZnGa_{2-x}O₄:xEr³⁺ (x=0.05) and ZnGa_{2-x}O₄:xEr³⁺ (x=0.01) phosphors were further confirmed by the measurement of pore size distribution, which was obtained by the nitrogen adsorption–desorption isotherm and Barrett–Joyner–Halenda (BJH) method, as shown in Figure 6 and Figure 7. The results of analyzes show that the presence of impurity Er ions leads to increased specific surface nanocrystalului of ZnGa₂O₄.

Table 1

Materials	Average pore radius of the adsorption (nm)	Average pore radius of the desorption (nm)	BET surface (m ² /g)	Total volume of pores (cc/g)
ZnGa ₂ O ₄	4.20	3.06	11.28	0.0249
ZnGa _{2-x} O ₄ :xEr ³⁺ x=0,05	4.23	3.36	11.43	0.0196
ZnGa _{2-x} O ₄ :xEr ³⁺ x=0,01	4.23	3.40	11.66	0.0230

Hydrothermal method is a successfully method for obtaining nanomaterials with a high degree of crystallinity and homogeneity of particles size.

4. Conclusions

Erbium - doped ZnGa₂O₄ phosphors with nominal formulae of ZnGa_{2-x}O₄:xEr³⁺ (x=0.05 and x=0.01) was synthesizes by hydrothermal method and characterizes structurally. From X-ray diffraction, spectra made with Anton Paar HTK2000 high-temperature camera is observe the spinels phase peaks (311) all nanomaterials (undoped and doped ZnGa₂O₄ with Er ions). From calculations using Scherrer's formula and from TEM measurements can be seen that the crystallite size is of nanometer and depends on the concentration of doping. Also, from TEM measurements can be seen the form cubic of the crystallization. The adsorption–desorption isotherms exhibits a type IV which is typically characteristic of mesoporous materials. When doped ZnGa₂O₄ with Er ions can see an improvement the value specific surface and it depends on the concentration of doped.

References

- [1] L. E. Shea, R. K. Datta, and Jr., J. J. Brown, J. Electrochem. Soc., **141**, 1950 (1994)
- [2] K. Hsu, M. Yang, and K. Chen, J. Mater. Sci: Mater. Electron., **9**, 283 (1998)
- [3] B. G. Tagiev, G. G. Guseinov, R. B. Dzhabbarov, O. B. Tagiev, N. N. Musaeva, A. N. Georgobiani, Inorg. Mater., **36**, 1189 (2000)
- [4] A. R. Phani, S. Santucci, S. Di Nardo, L. Lozzi, M. Passacantando, P. Picozzi, and C. Cantalini, J. Mater. Sci., **33**, 3969 (1998)

- [5] S.I. Mho, I.-K. Jeong, H. L. Park, *Solid State Commun.*, **105**, 179 (1998).
- [6] V. R. Kumar, K. V. Narasimhulu, N. O. Gopal, H. K. Jung, R. P. S. Chakradhar, J. L. Rao, *J. Phys. Chem. Solids*, **65**, 1367 (2004).
- [7] H. Naito, S. Fujihara, T. Kimura, *J. Sol–Gel Sci. Technol.* **26**, 997 (2003).
- [8] Z. Xu, Y. Li, Z. Liu, Z. Xiong, *Mater. Sci. Eng. B*, **110**, 302 (2004).
- [9] Y.S. Jeong, J.S. Kim, H.L. Park, *Solid State Communications* **139**, 157 (2006).
- [10] Z. Lou, J. Hao, *Thin Solid Films*, **450**, 334 (2004).
- [11] H.-W. Choi, B.-J. Hong, S.-K. Lee, K.-H. Kim, Y.-S. Park, *J. of Lumin.* **126**, 359 (2007).
- [12] J.S. Kim, J.S. Kim, T.W. Kim, S.M. Kim, H.L. Park, *Appl. Phys. Lett.* **86**, 091912 (2005)
- [13] M. Vasile, P. Vlazan, N. M. Avram, *J. of All. & Comp.* **500**, 185 (2010).
- [14] J. S. Kim, A. K. Kwon, J.S. Kim, H. L. Park, G. C. Kim, S. Han, *J. of Lumin.* **122–123**, 851 (2007)
- [15] M. Takesada, M. Osada, T. Isobe, *J. of Phy. & Chemis. of Solids*, **70(2)**, 281 (2009).
- [16] L. Wang, Z. Hou, Z. Quan, H. Lian, P. Yang, J. Lin, *Mat. Res. Bull.*, **44(10)**, 1978 (2009).
- [17] W. Zhang, J. Zhang, Y. Li, Z. Chen, T. Wang, *Applied Surface Science*, **256(14)**, 4702 (2010).
- [18] J.S. Kim, J.S. Kim, H.L. Park, *Solid State Commun.* **131**, 735 (2004).
- [19] J.S. Kim, H.I. Kang, W. N. Kim, J.I. Kim, J.C. Choi, H.L. Park, G.C. Kim, T.W. Ki, Y.H. Hwang, S.I. Mho, M.-C. Jung, M. Han, *Appl. Phys. Lett.* **82**, 2029 (2003)
- [20] M. Yu, J. Lin, Y.H. Zhou, S.B. Wang, *Mater. Lett.* **56**, 1012 (2002)
- [21] M. Vasile, P. Vlazan, P. Sfirloaga, I. Grozescu, N.M. Avram, E. Rusu, *Phys. Sc. T*, T135, 014046 (2009)
- [22] M. Vasile, N. Avram, P. Vlazan, I. Grozescu, M. Miclau, *J. Optoelectron. Adv. Mater.*, **10(11)**, 2898(2008)
- [23] M. Vasile, P. Vlazan, I. Grozescu, N. Avram, *Optoelectron. Adv. Mater. – Rapid Comm.*, **3(12)**, 1371 (2009)
- [24] S. Brauner, P.H. Emmett, E. Teller, *J. Am. Chem. Soc.*, **60**, 309 (1938)
- [25] T. Minami, H. Sato, K. Ohashi, T. Tomofuji, S. Takata, *J. Cryst. Growth* **117**, 370 (1992)

*Corresponding author: mihaela.vasile@icmct.uvt.ro